Extraordinary Hall effect in $(Ni_{80}Fe_{20})_x(SiO_2)_{1-x}$ thin films

Hui Liu, Fuk Kay Lee, Rong Kun Zheng, X. X. Zhang, and Ophelia K. C. Tsui*
Department of Physics and Institute of Nano Science and Technology, Hong Kong University of Science and Technology, Clear Water Bay, Kowloon, Hong Kong

(Received 16 April 2004; revised manuscript received 26 July 2004; published 27 December 2004)

The extraordinary Hall effect (EHE) in ferromagnetic samples is generally attributed to scatterings of iterant electrons in the presence of spin-orbit interactions. In this work, our study of the thickness dependence of the EHE in the $(Ni_{80}Fe_{20})_x(SiO_2)_{1-x}$ system showed the spontaneous Hall resistivity, ρ_{xy}^S to be quite independent of the film thickness while the Hall coefficient, R_S ($\equiv \rho_{xy}^S/M_S$, where M_S is the saturated magnetization), increased monotonically owing to a depression in M_S. We point out that the independence of ρ_{xy}^S with reducing thickness could arise if the morphological structure of the sample becomes two dimensional with decreasing film thickness, which is expected from classical percolation theory. We also find in the $(Ni_{80}Fe_{20})_x(SiO_2)_{1-x}$ system (with varying x) that $\rho_{xy}^S \propto \rho_{xx}^\gamma$ where $\gamma = 0.53$, which disagrees with the value of 2 frequently attributed to the side jump effect, but which can be explained in terms of the more general form $\rho_{xy}^S = \rho_{xx}\Delta_{ye}/\Lambda_{SO}$, where Δ_{ye} is the side jump displacement and Λ_{SO} is the spin-orbit mean free path.

DOI: 10.1103/PhysRevB.70.224431 PACS number(s): 75.70.−i, 73.50.−h

I. INTRODUCTION

Extensive studies have been carried out on heterogeneous magnetic multilayers and granular systems for their potential application as giant magnetoresistance materials. It is well documented that surface and interface scatterings could have strong effects on the magnetotransport properties of these systems.[1–6] In typical approaches to studying the effect of surface scatterings, the sample thickness is usually decreased[1,2,4,6] or the average magnetic domain size[1–3] and the resultant changes in the magnetotransport properties are determined. Magnetic granular samples require special attention, however. As their average grain size and film roughness usually undergo distinctive changes as the sample thickness is reduced towards the average grain size in bulk (which is typically 1 to ~10 nm), additional electron scatterings caused by reducing the sample thickness could come from changes in the metal grain size and the surface roughness of the sample, if any, with decreasing film thickness. We would thus call the additional scatterings from reducing the sample thickness "effective surface scatterings" (as opposed to simply "surface scatterings," which has been more generally referred to).

Our original goal in this study was to analyze the effective surface scatterings in $Ni_{80}Fe_{20}$ and granular $(Ni_{80}Fe_{20})_x(SiO_2)_{1-x}(x=0.7)$ sputtered films (both covered by SiO_2) by measuring the changes in their extraordinary Hall signals with decreasing film thickness from 30 to 2 nm. The extraordinary Hall effect (EHE) is especially suited for use as a monitor of effective surface scattering because it is the most sensitive to electron scatterings amongst all magnetic properties.[3,7] Our results reveal that the Hall coefficient, R_S, of both $Ni_{80}Fe_{20}$ and $(Ni_{80}Fe_{20})_{0.7}(SiO_2)_{0.3}$ increased by 3–4 times with this thickness reduction, but the spontaneous Hall resistivity, ρ_{xy}^S changed relatively little. We determined that the increase in R_S has little to do with the increase in the effective surface scatterings, but is due, instead, to a fourfold depression in the saturated magnetization, M_S of both $Ni_{80}Fe_{20}$ and $(Ni_{80}Fe_{20})_{0.7}(SiO_2)_{0.3}$ with decreasing thickness. The significantly smaller change in ρ_{xy}^S is understandable from the results of classical percolation theory that the ρ_{xy}^S of a metal-insulator composite should become constant as the sample structure becomes two-dimensional (2D).[8–11] We confirm this 2D phenomenon in $(Ni_{80}Fe_{20})_x(SiO_2)_{1-x}$ by showing that a plateau in ρ_{xy}^S indeed occurs as thin films of $(Ni_{80}Fe_{20})_x(SiO_2)_{1-x}$ (with fixed thickness of 30 nm) approach the percolation threshold (through reduction of the metal volume fraction, x) at which the percolation correlation length diverges.[8] Finally, we discuss issues concerning the interpretation of Berger's result for side-jump effects,[12] which is commonly used to analyze EHE data from resistive ferromagnets.

II. EXPERIMENT

$Ni_{80}Fe_{20}$ and granular $(Ni_{80}Fe_{20})_x(SiO_2)_{1-x}$ films were prepared using a magnetron dc sputtering system as described elsewhere.[13–15] A 100-nm-thick SiO_2 capping layer was sputtered on top of all films to protect them from further oxidation. The thickness of the films was controlled by a crystal balance monitor mounted near the sample surface inside the sputtering chamber. The samples were lithographically patterned into 1 mm × 6 mm rectangles with six terminals: two for carrying the current, two for measuring the longitudinal voltage, and two for measuring the transverse voltage. To eliminate spurious signals due to the Seebeck effect, the longitudinal voltage was measured twice with the dc current reversed between the measurements. Then, the difference between the two voltages was divided by 2 to obtain the resistive potential difference across the sample. The Hall signal was deduced from the asymmetric component of the transverse voltage $V_{xy,\mathrm{asy}}$ versus the magnetic field H between −5 and 5 T. The Hall resistivity, ρ_{xy}, was calculated from $V_{xy,\mathrm{asy}}h/I$, where h is the sample thickness and I is the applied dc current.

For ferromagnetic conductors,

$$\rho_{xy} = R_0[H + 4\pi M(1 - D)] + 4\pi R_S M, \quad (1)$$

where R_0 is the ordinary Hall coefficient, M the magnetization, D the demagnetization factor, and R_S the extraordinary Hall coefficient. Since the applied magnetic field is perpendicular to the film surface in all field dependent measurements, D is close to 1. In Eq. (1), the first term comes from the classical Lorentz force, whereas the second term is generally attributed to the EHE, believed to be due to spin-orbit scatterings.[12,16,17] To determine R_S, the extrapolated value of ρ_{xy} at zero magnetic field (denoted by ρ_{xy}^S) from the region where the magnetization saturates is divided by the saturated magnetization, M_S, i.e.,

$$R_S = \rho_{xy}^S / M_S. \quad (2)$$

The magnetization was measured with a Quantum Design superconducting quantum interference device magnetometer. Samples for transmission electron microscopy (TEM) and atomic force microscopy (AFM) imaging were prepared as described above for electrical measurements but without the SiO_2 capping layer. These samples were deposited on carbon-coated TEM grids and glass, respectively. Bright-field TEM micrographs were obtained by a Philips C-M20 model TEM. Atomic force microscopic topographical images of the samples were obtained by a Seiko Instruments (Chiba, Japan) SPA-300HV model AFM operated in the dynamic force mode.

III. RESULTS AND DISCUSSIONS

Shown in Figs. 1(a) and 1(b) are plots of the extraordinary Hall (EH) coefficient R_S versus the film thickness h for the $Ni_{80}Fe_{20}$ and $(Ni_{80}Fe_{20})_{0.7}(SiO_2)_{0.3}$ films, respectively, at a temperature of $T = 5$ K. For both materials, the R_S acquires its bulk value for $h \geqslant 30$ nm with the value for $(Ni_{80}Fe_{20})_{0.7}(SiO_2)_{0.3}$ a factor of 6 larger than that for $Ni_{80}Fe_{20}$. This enhancement of R_S in $(Ni_{80}Fe_{20})_x(SiO_2)_{1-x}$ with respect to that in pure $Ni_{80}Fe_{20}$ is associated with the giant Hall effect (GHE) demonstrated in ferromagnetic metal-insulator composites[13–15,18,19] in which the EH effect demonstrates a 10^3–10^4-fold enhancement near the percolation threshold of the composites. While the origin of the GHE is so far not fully understood,[13–15,18,19] an order-of-magnitude estimate[14] showed that the magnitude of enhancement is too large to come from a divergence of the Hall resistivity at the 3D percolation threshold.[8] Most probably, the GHE has to do with additional electron scatterings caused by the ferromagnetic metal-insulator interfaces and the higher degree of disorder inside the metal grains in approaching the percolation limit, in keeping with the spin-orbit nature of the EHE.[12,16,17] This view is in good accord with previous findings that the GHE was significantly reduced by annealing the granular sample at high temperatures[14] whereupon the average size of the metal grains increased and the degree of disorder in the metal likely improved as well.

Shown in Figs. 2(a) and 2(b) are plots of the longitudinal resistivity, ρ_{xx}, normalized to the resistivity at 5 K versus the logarithm of temperature T for the $Ni_{80}Fe_{20}$ and the

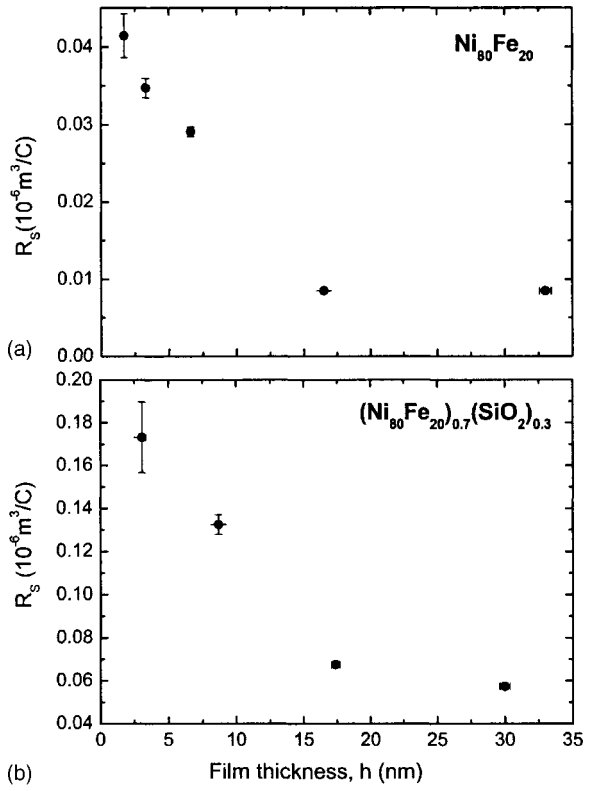

FIG. 1. The extraordinary Hall coefficient, R_S vs film thickness h for (a) the $Ni_{80}Fe_{20}$ and (b) the $(Ni_{80}Fe_{20})_{0.7}(SiO_2)_{0.3}$ films at 5 K.

$(Ni_{80}Fe_{20})_{0.7}(SiO_2)_{0.3}$ films, respectively, with different thicknesses. In both types of films, the evolution of the $\rho_{xx} - T$ curves with decreasing thickness is similar, resembling the generic metal-to-insulator transition found in $(Ni_{80}Fe_{20})_x(SiO_2)_{1-x}$ with decreasing metal fraction x.[13,19] In metallic samples, the temperature coefficient of resistivity (TCR) is positive from 5 to 300 K; in insulating samples, tunneling conduction[20,21] prevails and the TCR is negative; but in the intermediacy between these two extremes, the TCR may change from negative, exhibiting a $-\log T$ dependence at low temperatures, to positive at high temperatures. This temperature dependence has been postulated[19] to arise from the nanometer-sized metal grains (that have electronic energy quantizations close to the thermal energy at room temperature) reaching such an abundance as to be able to block enough of the conduction paths inside the sample to cause a negative TCR at low temperatures but not at high temperatures. From the results of Figs. 2(a) and 2(b), it is apparent that both types of films become less conducting with decreasing film thickness. The metal-to-insulator transition does not occur until $h \approx 3$ nm, however, which is notably less than the thickness where R_S begins to increase with decreasing thickness (i.e., 15 nm, Fig. 1).

We examined the morphological changes, if any, occurring to the two films with decreasing film thickness. Shown in Figs. 3(a) and 3(b) are bright-field TEM micrographs of the $Ni_{80}Fe_{20}$ and $(Ni_{80}Fe_{20})_{0.7}(SiO_2)_{0.3}$ films, respectively, with different thicknesses from ~30 to

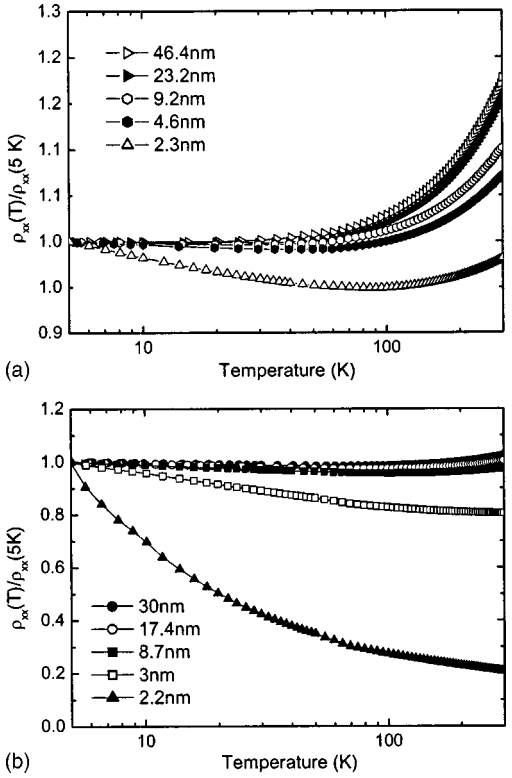

FIG. 2. Semilogarithmic plots of longitudinal resistivity normalized to the values at 5 K vs temperature for (a) the $Ni_{80}Fe_{20}$ and (b) the $(Ni_{80}Fe_{20})_{0.7}(SiO_2)_{0.3}$ films with different thicknesses.

$\sim$3 nm. As seen, with decreasing film thickness, the average metal grain size decreases with the granules clumping together to form increasingly sharpened islands that are about $\sim$10 nm laterally in size. To confirm the formation of islands, we examined the topography of the films by AFM. Shown in Fig. 4 are the AFM topographical images of $Ni_{80}Fe_{20}$ films with thicknesses from 33 nm to 1.7 nm. Beneath each image is the cross-sectional profile along an arbitrary line drawn in the image as shown. With decreasing film thickness, the film roughens with the obvious formation of islands. In the films with thickness below 15 nm, the average height of the islands is taller than the nominal film thickness. At $h<6.6$ nm, the islands become clearly isolated. The $(Ni_{80}Fe_{20})_{0.7}(SiO_2)_{0.3}$ films demonstrated similar topographical variations with decreasing thickness as did the $Ni_{80}Fe_{20}$ films.

Magnetic properties of nanostructures are known to vary strongly with local structures including feature size,[3,7,22] interfacial condition,[1,5,23,24] and disorder.[25,26] Table I gives the measured values of M_S at 5 K of the same $Ni_{80}Fe_{20}$ and $(Ni_{80}Fe_{20})_{0.7}(SiO_2)_{0.3}$ films studied in Fig. 1. As seen, M_S decreases systematically with decreasing film thickness in both types of films. It is noteworthy that the M_S of the 30-nm $(Ni_{80}Fe_{20})_{0.7}(SiO_2)_{0.3}$ film is only 53% of that of the $Ni_{80}Fe_{20}$ film with similar thickness, which cannot be accounted for by the difference in their volume fraction in the ferromagnetic component $Ni_{80}Fe_{20}$.[27] By correlating this result with the TEM and AFM images shown in Figs. 3 and 4, we suggest that the smaller values of M_S in our films are from the smaller average metal grain sizes and perhaps also from the greater surface roughness. Reduction of M_S with decreasing sample size has been found in spherical Fe_3O_4 nanoparticles[28] and (111)-oriented $Y_3Fe_5O_{12}$ thin films.[29] On the other hand, M_S was reportedly constant with variations of the Co domain size in $Co_{20}Ag_{80}$ (Ref. 3) and with thickness reduction in Ni films,[30] both to the nanometer range. Apparently, variations in M_S with sample size depend on numerous factors as stipulated previously[1,3,5,7,22–26] and cannot be easily generalized. We also measured the M_S in a series of $(Ni_{80}Fe_{20})_x(SiO_2)_{1-x}$ films with different metal fractions x but fixed $h\approx 30$ nm (data not shown). We found that M_S decreased by an order of magnitude as x decreased from 1 to $\sim$0.4, with large fluctuations in M_S (between 50 and 209 emu/cm^3) occurring around $x=0.5\pm0.1$, in the vicinity of the percolation threshold. This order of magnitude decrease in M_S with x decreasing from 1 through the percolation threshold is consistent with the decrease found in the $Ni_{80}Fe_{20}$ and $(Ni_{80}Fe_{20})_x(SiO_2)_{1-x}$ films upon reducing their thickness from 30 to 3 nm (Table I), where their $\rho_{xx}-T$ curves (Fig. 2) demonstrate the metal-to-insulator transition. This result supports the argument that the variations in M_S shown in Table I of $(Ni_{80}Fe_{20})_x(SiO_2)_{1-x}$ films reflect structural changes inside the films.

A theorem was well established in 2D conductor-insulator binary networks that the Hall resistivity of any one such

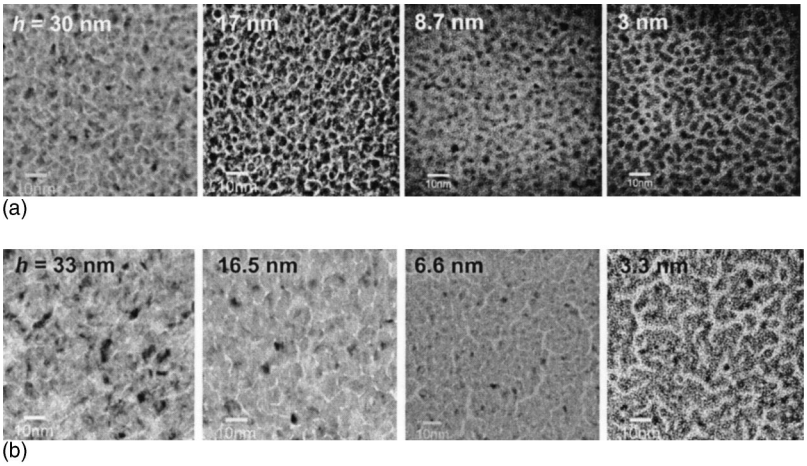

FIG. 3. Transmission electron micrographs of the (a) $Ni_{80}Fe_{20}$ films and (b) $(Ni_{80}Fe_{20})_{0.7}(SiO_2)_{0.3}$ films with different thicknesses h as indicated.

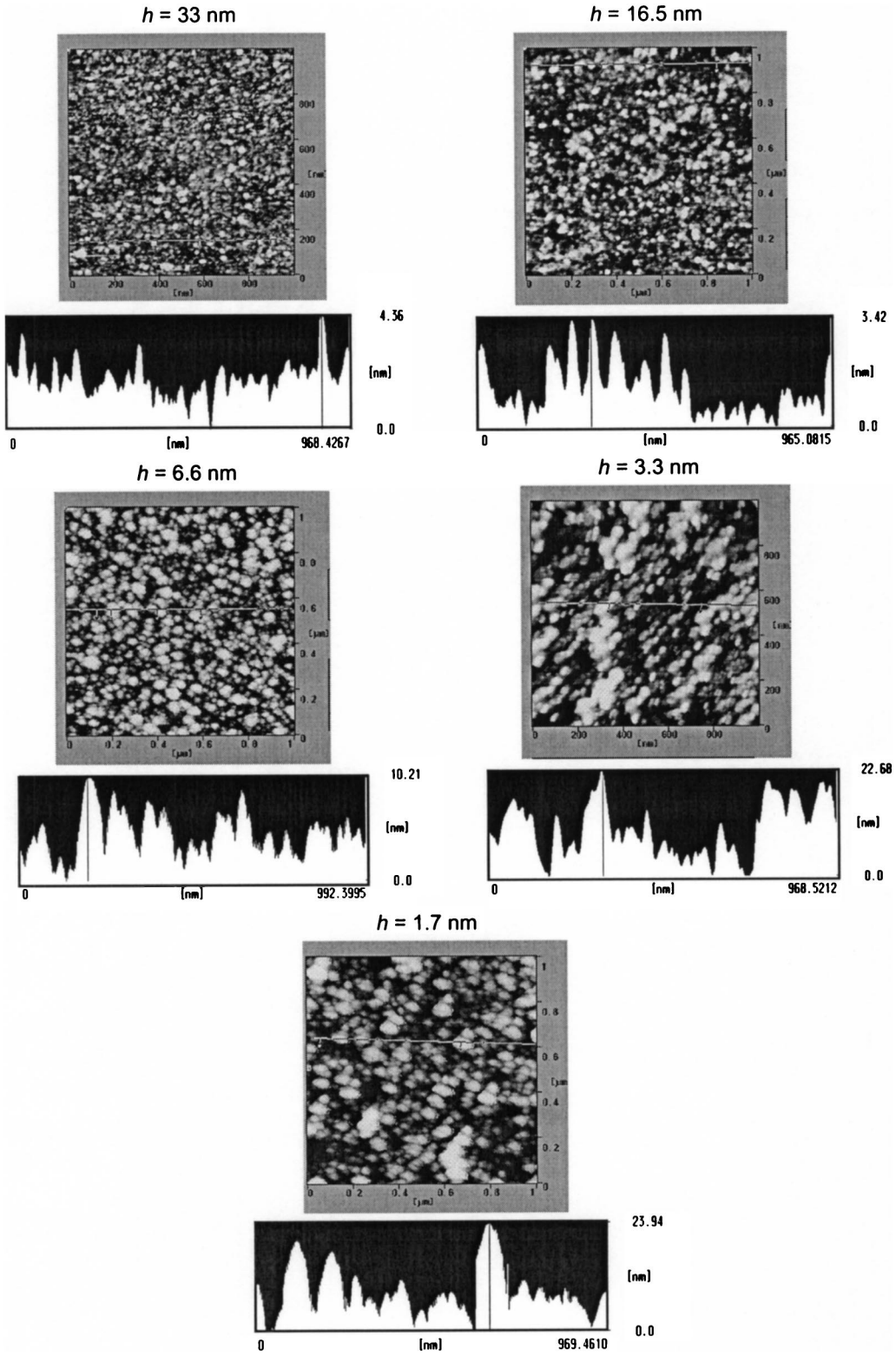

FIG. 4. AFM topographical micrographs of $Ni_{80}Fe_{20}$ films with different thicknesseses from 33 to 1.7 nm. Immediately underneath each micrograph is the cross-sectional profile along an arbitrary line drawn on the micrograph as shown.

network is constant (independent of the conductor fraction), equal to the Hall resistivity of the conductor composing the network when in bulk.[8–11] Our results may imply that our films become 2D with decreasing film thickness (Fig. 4) such that the ~fourfold increase in R_S ($\equiv \rho_{xy}^S / M_S$) displayed in Fig. 1 could arise from the decrease in M_S shown in Table I. In Fig. 5, ρ_{xy}^S versus the film thickness is plotted for the same films studied in Fig. 1. The ρ_{xy}^S of the $Ni_{80}Fe_{20}$ films is essentially constant from $h=30$ to 1.7 nm, consistent with expectations from the 2D theorem.[8–11] A previous study of

TABLE I. Measured values of saturated magnetization, M_S of $Ni_{80}Fe_{20}$ and $(Ni_{80}Fe_{20}(SiO_2)_{0.3}$ films with different thicknesses, h at 5 K.

Sample	h (nm)	M_S (emu/cm^3)
$Ni_{80}Fe_{20}$	33	560±7
	16.5	494±9
	3.3	152±5
	1.7	122±8
$(Ni_{80}Fe_{20})_{0.7}(SiO_2)_{0.3}$	30	290±4
	17.4	237±4
	8.7	147±5
	3	66±6

evaporated Ni films also showed ρ_{xy}^S as constant when the film thickness was reduced to 5–6 nm,[6] which could also be a result of the 2D theorem. In the $(Ni_{80}Fe_{20})_{0.7}(SiO_2)_{0.3}$ films, ρ_{xy}^S is constant only until $h=17.4$ nm. The ρ_{xy}^S of the 8.7- and 3-nm films deviate by 22% and 50%, respectively, from that of the thicker films. In these $(Ni_{80}Fe_{20})_{0.7}(SiO_2)_{0.3}$ films, where discrete islands are formed with heights greater than or comparable to the film thickness (Fig. 4), we believe the 2D theorem[8–11] could break down as these films may no longer be treated as binary conductor-insulator networks (meaning that all the conducting regions of the network have the same transport properties), which is a prerequisite of the 2D theorem.[11] Due to the thickness variations, the conducting regions of these films, as $(Ni_{80}Fe_{20})-(SiO_2)$ networks, could vary quite significantly from region to region in microscopic structure and/or even the composition of $Ni_{80}Fe_{20}$ inside the conducting region, causing large variations in the transport properties of different conducting regions and violation of the prerequisite of the 2D theorem. In the following we show how the 2D theorem may be demonstrated in $(Ni_{80}Fe_{20})_x(SiO_2)_{1-x}$.

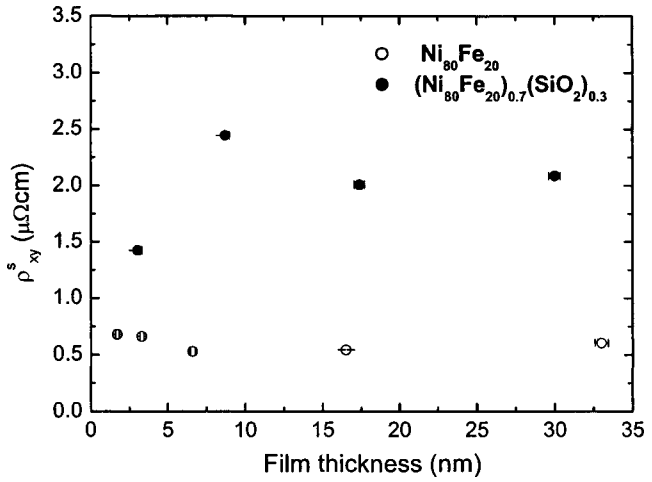

FIG. 5. Plots of ρ_{xy}^S vs film thickness of $Ni_{80}Fe_{20}$ films (open circles) and $(Ni_{80}Fe_{20})_{0.7}(SiO_2)_{0.3}$ films (solid circles). The ρ_{xy}^S data are obtained by multiplying the R_S data of Fig. 1 by the measured M_S of the respective film.

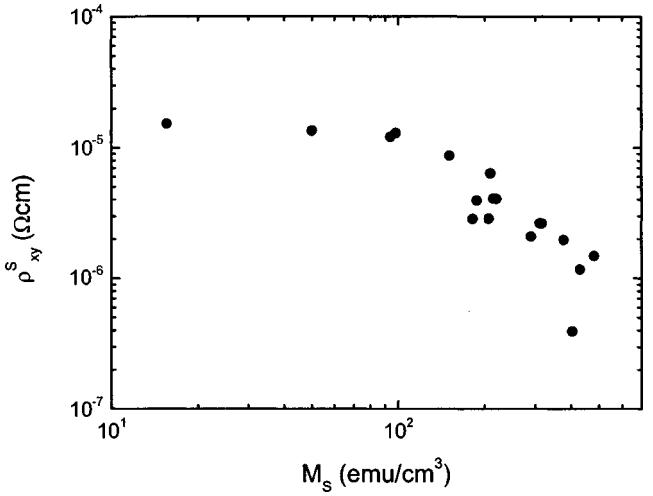

FIG. 6. A plot of ρ_{xy}^S vs M_S of $(Ni_{80}Fe_{20})_{0.7}(SiO_2)_{0.3}$ films with different x but fixed thickness equal 30 nm.

In granular metal-insulator composite films, a crossover from 3D to 2D behaviors always takes place as the percolation threshold is approached[31,32] whereupon the percolation correlation length diverges[8] and becomes larger than the film thickness. This provides a convenient way to study the 2D theorem in $(Ni_{80}Fe_{20})_x(SiO_2)_{1-x}$ by reducing the metal fraction x. Shown in Fig. 6 is the measured ρ_{xy}^S of $(Ni_{80}Fe_{20})_x(SiO_2)_{1-x}$ films with h fixed at ~30 nm [where the film roughness is <10% of the film thickness (Fig. 4)], and different metal fractions x, are plotted against M_S. A plateau of ρ_{xy}^S is clearly evident around $50 \leqslant M_S \leqslant 209$ emu/cm^3, which is where the percolation threshold is. It is also interesting to note that the ρ_{xy}^S of our films never rises above 10^2 times the value of the pure metal film, although a GHE enhancement of more than 10^3 times has been reported for this system near $x=0.56$.[13,15,18] The discrepancy can be understood from the thickness of the films employed in this experiment (~30 nm) being thinner than in the earlier studies (≈1 μm),[13,15,18] so that our films become 2D sooner, forcing ρ_{xy}^S to level off due to the 2D theorem before the GHE develops to its full strength.

In passing, we discuss why the 2D theorem should only apply to ρ_{xy}^S (i.e., the extraordinary Hall resistivity at saturated magnetization), but not the extraordinary Hal resistivity at a fixed magnetic field in ferromagnetic granular materials or the extraordinary Hall coefficient R_S. As mentioned above, the 2D theorem only applies to metal-insulator networks that are binary.[11] With the Hall resistivity of these substances coming from the EHE, which in turn comes from scatterings of the iterant electrons in the presence of spin-orbit interactions, the Hall resistivities of individual domains depend on the spin orientations of each domain with respect to the direction of the applied dc current. As a result, before the spins of all domains are aligned, the Hall resistivities of different domains could be very different, invalidating the precondition of the 2D theorem. Furthermore, since the sample magnetization generally contains contributions from magnetic moments of both free and bound charges, a proper normalization of the spontaneous

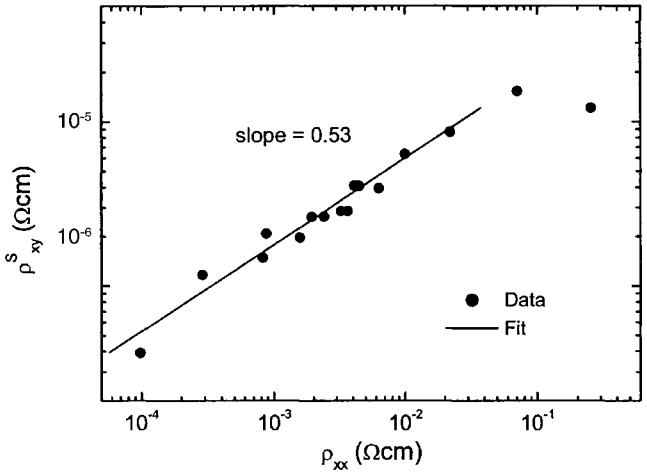

FIG. 7. The spontaneous Hall resistivity ρ^S_{xy} of $(Ni_{80}Fe_{20})_{0.7}(SiO_2)_{1-x}$ films with different x plotted against ρ_{xx} on the log-log scale. The data were obtained at 5 K. The value of x was varied across the percolation threshold. The solid line is the best linear fit to the data for ρ_{xx} below 0.02 Ω cm. Its slope was found to be 0.53.

Hall signal should entail division of ρ^S_{xy} by the component of magnetization coming solely from the free charges. Hence, the EH coefficient R_S obtained by dividing ρ^S_{xy} by the total magnetization may thus not always provide the proper normalization for the spontaneous Hall signal. It should therefore be emphasized that ρ^S_{xy} not R_S, should be used as the measure of EHE.

The effect of electron scatterings on the EHE of heterogeneous magnetic systems is often analyzed by examining the $\rho_{xy} \propto \rho^{\gamma}_{xx}$ scaling relation (where γ is the scaling exponent). Prevalent theories[12,16,15] suggest that spontaneous Hall signals arise from spin-orbit scatterings of the iterant electrons by the positive ions resulting in asymmetric deflections (i.e., the so-called skew scatterings[17]) and/or discontinuous sideways displacements of the iterant electrons (i.e., the so-called side-jump effect).[12] It is generally believed that skew scatterings lead to $\rho^S_{xy} \propto \rho_{xx}$ while the side-jump effect leads to $\rho^S_{xy} \propto \rho^2_{xx}$, with the side-jump effect dominating when ρ_{xx} is large. Among the various heterogeneous magnetic systems studied recently, however, serious disagreement has been found in these theoretical predictions.[33] For the samples studied here [which are granular networks of $Ni_{80}Fe_{20}$—notably a heavily (Fe-) doped alloy of Ni—and hence are resistive], we expect the side-jump effect to dominate. We found $\rho^S_{xy} \propto \rho^{0.53}_{xx}$ at 5 K before ρ^S_{xy} comes to a plateau (Fig. 7; ρ_{xx} was varied by varying x), which also disagrees with theoretical predictions.

In the original derivation by Berger,[12] the expression for the Hall resistivity due to the side-jump effect for a single band of carriers is

$$\rho^S_{xy} = \frac{\rho_{xx}\Delta y_e}{\Lambda_{SO}}, \tag{3}$$

where Δy_e is the sideway displacement of the electrons due to spin-orbit scatterings and Λ_{SO} is the electron spin-orbit scattering meanfreepath. By assuming that $\rho_{xx} \propto \Lambda_{SO^{-1}}$, Berger deduced the well-known result, $\rho^S_{xy} \propto \rho^2_{xx}$. However, the presumption that $\rho_{xx} \propto \Lambda_{SO^{-1}}$ is equivalent to assuming that the number of spin-orbit scattering events is proportional to the number of electron collisions, which is generally not valid except when the spin-orbit scatterings and electron collisions are predominantly caused by the same scatterers. With dirty systems like ours, further addition of scatteres to the system (including impurities, disorders and phonons) would generally change the electron collision rate and the spin-orbit scattering rate differently, depending on the quantity and nature of the preexisting scatterers. Table II compares the values of ρ^S_{xy} and ρ_{xx} found in Ni, $Ni_{80}Fe_{20}$ and $(Ni_{80}Fe_{20})_{0.7}(SiO_2)_{0.3}$. It is apparent that the Fe additions are much more effective in enhancing ρ^S_{xy} than are the SiO_2 inclusions whereas the SiO_2 inclusions are a little more effective in increasing ρ_{xx}. This observation together with the vastly smaller values of ρ^S_{xx} and ρ_{xx} in Ni than in $Ni_{80}Fe_{20}$ may explain why both ρ^S_{xy} and ρ_{xx} of our samples were little affected by thickness reduction between $h \approx 30$ nm and 15 nm prior to discrete island formation, whereas an approximately quadratic rise in ρ^S_{xy} with ρ_{xx} was apparent in pure Ni (Ref. 6) as the film thickness was decreased over a similar range. Evidently, additional effective surface scatterings due to morphological changes in the films by thickness reduction readily dominated the preexisting scatterers in pure Ni films (for both spin-orbit scatterings and electron collisions) but not in $(Ni_{80}Fe_{20})_x(SiO_2)_{1-x}$ ($x=1$ or 0.7) films in which the existing scatterers from the Fe and/or SiO_2 inclusions are quite strong (according to Table II).

TABLE II. Comparison between values of ρ^S_{xy} and ρ_{xx} for bulk Ni, $Ni_{80}Fe_{20}$ and $(Ni_{80}Fe_{20})_{0.7}(SiO_2)_{0.3}$

Sample	ρ^S_{xy} ($\mu\Omega$ cm)	ρ_{xx} ($\mu\Omega$ cm)
Ni (from Ref. 6)	0.025	6.5
$Ni_{80}Fe_{20}$	0.5	100
$(Ni_{80}Fe_{20})_{0.7}(SiO_2)_{0.3}$	3	2000

With $\gamma=0.53$ (<1) as shown in Fig. 7, Eq. (3) implies that $\Delta y_e/\Delta_{SO}$ decreases with the addition of SiO_2 to $(Ni_{80}Fe_{20})_x(SiO_2)_{1-x}$ which may seem counterintuitive if one assumes, as Berger did,[12] that Δy_e is a constant. Nevertheless, one might foresee subsidiary effects that could make Δy_e variable and/or Δ_{SO} increase with addition of SiO_2 in $(Ni_{80}Fe_{20})_x(SiO_2)_{1-x}$. For example, the added heterogeneity and disorder from SiO_2 addition could change the velocity and density of electrons, which might in turn change the spin-orbit scattering rate. (The former could affect the scattering rate through its possible effect on the scattering cross-section.) In samples exhibiting tunneling conduction, there could be localization effects on the electron scatterings. The increased magnetic disorder implied by the reduction of M_S with increasing SiO_2 concentration and decreasing sample thickness may add new dimensions to the scattering problem. Conventional wisdom assumes that temperature affects EHE through its effect on the density of phonons, which are usually regarded as a kind of scatterer. Thus the same $\rho^S_{xy} - \rho_{xx}$ relation is expected to hold whether ρ_{xx} is varied throught the

temperature or the concentration of the foreign substance added. But for the subsidiary effects discussed above, changes in the temperature should affect electron scatterings in vastly different ways than changes in the concentration of the added insulating material. In general, the $\rho_{xy}^{S}-\rho_{xx}$ relations obtained by varying the temperature and by changing the amount of extrinsic inclusions (or the sample thickness) may differ by a great deal. We believe this difference could be the reason behind the unusual value of γ (=0.53) presently found in $(Ni_{80}Fe_{20})_x(SiO_2)_{1-x}$ and the wide range of γ reported in the literature.[33]

IV. CONCLUSION

We have investigated the extraordinary Hall effect in $(Ni_{80}Fe_{20})_x(SiO_2)_{1-x}$ thin films and have concentrated on several rarely discussed issues. First, ρ_{xy}^{S} not R_S is the fundamental quantity that should be used for the measure of extraordinary Hall effect. In thickness dependence studies, additional scatterings arising from reducing the sample thickness should include not only scatterings from the film boundaries but also those due to changes in the graininess and roughness of the films, which we call the effective surface scatterings throughout this paper. In general, the significance of the effects from effective surface scatterings is dependent on both the density and the nature of the scatterers preexisting in the system, and it can be different for ρ_{xy}^{S} and ρ_{xx}. Should the system change from 3D to a 2D granular network either from discrete island formation or from the percolation correlation length becoming larger than the sample thickness, the spontaneous Hall resistivity should come to a plateau value equal to the spontaneous Hall resistivity of the conducting regions. We also discussed the much-cited $\rho_{xy}\propto\rho_{xx}^{2}$ from Berger's result for side-jump effects. We emphasize the importance of preserving the original form derived by Berger, i.e., $\rho_{xy}=\rho_{xx}\Delta y_e/\Lambda_{SO}$, in separating the electron mean-free-path from the spin-orbit mean-free-path, which seems to have been largely neglected. Experimentally, the ρ_{xy} versus ρ_{xx} relation is often investigated by varying the temperature. If variations in the temperature do more than just adding phonons to the system, prospects of its effects on the electron and spin-orbit mean free paths must be assessed before a realistic interpretation of the relation between ρ_{xy} and ρ_{xx} can be made.

ACKNOWLEDGMENTS

We are indebted to Professor Ping Sheng for valuable discussions and ongoing support. Without his support and encouragement, this work would not have been finished. We would also like to acknowledge the assistance of Microelectronics Fabrication Facility and Materials Characterization & Preparation Facility at HKUST in sample preparation and characterization. Financial support from the Research Grants Council of Hong Kong under Project Nos. HKUST6150/01P and HKUST6165/01P was important to this study.

*Author to whom correspondence should be addressed. Email address: phtsui@ust.hk

[1] R. J. Hicken, G. T. Rado, G. Xiao, and C. L. Chien, Phys. Rev. Lett. **64**, 1820 (1990).
[2] S. N. Song, C. Sellers, and J. B. Ketterson, Appl. Phys. Lett. **59**, 479 (1991).
[3] P. Xiong, G. Xiao, J. Q. Wang, J. Q. Xiao, J. S. Jiang, and C. L. Chien, Phys. Rev. Lett. **69**, 3220 (1992).
[4] J. -Q. Wang, G. Xiao, Phys. Rev. B **51**, 5863 (1995).
[5] V. Korenivski, K. V. Rao, J. Colino, and I. K. Schuller, Phys. Rev. B **53**, R11 938 (1996).
[6] A. Gerber, A. Milner, L. Goldshmit, M. Karpovski, B. Lemke, H.-U. Habermeier, and A. Sulpice, Phys. Rev. B **65**, 054426 (2002).
[7] J. C. Denardin, A. B. Pakhomov, A. L. Brandl, L. M. Socolovsky, M. Knobel, and X. X. Zhang, Appl. Phys. Lett. **82**, 763 (2003).
[8] D. J. Bergman and D. Stroud, Solid State Phys. **46**, 147 (1992).
[9] H. J. Juretschke, R. Landauer, J. A. Swanson, J. Appl. Phys. **27**, 836 (1956).
[10] A. Palevski, M. L. Rappaport, A. Kapitulnik, A. Fried, and G. Deutscher, J. Phys. (France) Lett. **45**, L-367 (1984)
[11] D. Stroud, and D. J. Bergman, Phys. Rev. B **30**, 447 (1984).
[12] L. Berger, Phys. Rev. B **2**, 4559 (1970).
[13] A. B. Pakhomov, X. Yan, and B. Zhao, Appl. Phys. Lett. **67**, 3497 (1995).
[14] X. N. Jing, N. Wang, A. B. Pakhomov, K. K. Fung, and X. Yan, Phys. Rev. B **53**, 14 032 (1996).
[15] A. B. Pakhomov and X. Yan, Y. Xu, J. Appl. Phys. **79**, 6140 (1996).
[16] J. Smit, Physica (Amsterdam) **21**, 877 (1955).
[17] J. Smit, Physica (Amsterdam) **24**, 39 (1958).
[18] A. B. Pakhomov, S. K. Wong, X. Yan, and X. X. Zhang, Phys. Rev. B **58**, R13 375 (1998).
[19] A. B. Pakhomov, X. Yan, N. Wang, X. N. Jing, B. Zhao, K. K. Fung, J. Xhie, T. F. Hung, and S. K. Wong, Physica A **241**, 344 (1997).
[20] N. F. Mott, Philos. Mag. **91**, 835 (1969).
[21] P. Sheng, B. Abeles, and Y. Arie, Phys. Rev. Lett. **31**, 44 (1973).
[22] S. I. Woods, J. R. Kirtley, S. Sun, and R. H. Koch, Phys. Rev. Lett. **87**, 137205 (2001).
[23] F. C. Voogt, T. Fujii, P. J. M. Smulders, L. Niesen, M. A. James, and T. Hibma, Phys. Rev. B **60**, 11 193 (1999).
[24] D. M. Schaller, D. E. Bürgler, C. M. Schmidt, F. Meisinger, and H.-J. Güntherodt, Phys. Rev. B **59**, 14 516 (1999).
[25] T. Hibma, F. C. Voogt, L. Niesen, P. A. A. van der Heijden, W. J. M. de Jonge, J. J. T. M. Donkers, and P. J. Vander Zaag, J. Appl. Phys. **85**, 5291 (1999).
[26] M. P. Morales, M. Andres-Verges, S. Veintemillas-Verdaguer, M. I. Montero, and C. J. Serna, J. Magn. Magn. Mater. **203**, 146 (1999).
[27] One possible reason for the reduction of M_S in the $(Ni_{80}Fe_{20})_x(SiO_2)_{1-x}$ composite is the formation of antiferro-

magnetic FeO or NiO surface layers around the magnetic domains.

[28] G. F. Goya, T. S. Berquó, F. C. Fonseca, and M. P. Morales, J. Appl. Phys. **94**, 3520 (2003).

[29] T. Takeuchi, and Y. Sugita, J. Appl. Phys. **59**, 2925 (1986).

[30] C. A. Neugebauer, Phys. Rev. **116**, 1441 (1959).

[31] A. Kapitulnik, and G. Deutscher, Phys. Rev. Lett. **49**, 1444 (1982)

[32] A. Kapitulnik, and G. Deutscher, J. Phys. A **16**, L255 (1983).

[33] The introduction of Ref. 6 contains a summary on the incoherent results of y in the literature.